View metadata, citation and similar papers at core.ac.uk
brought to you by CORE
provided by Xiamen University Institutional Repository

phys. stat. sol. (a) **196**, No. 2, 450–458 (2003) / **DOI** 10.1002/pssa.200306453

Electrical properties of oxide-coated metal (Co, Cr, Ti) cluster assemblies

D. L. Peng[*], **T. Hihara,** and **K. Sumiyama**

Department of Materials Science and Engineering, Nagoya Institute of Technology, Nagoya 466-8555, Japan

Received 24 April 2002, revised 7 January 2002, accepted 14 January 2003
Published online 31 March 2003

PACS 73.63.–b

Oxide-coated metal (Co, Cr and Ti) cluster assemblies whose mean cluster sizes are 8–13 nm have been fabricated by a plasma-gas-condensation type cluster beam deposition technique. With increasing oxygen gas flow rate R_{O_2}, the oxide-coated metal cluster-assembled films exhibit a metal–nonmetal transition. In the metallic regime, the resistivity reveals ln T dependence at low temperature due to weak localization of conduction electrons and/or electron–electron interactions in the disordered oxide-coated cluster-assembled films. The ln T dependence still remains for the very thick oxide-coated metal-cluster-assembled films (the actual thickness t_c = 2400 nm) which is clearly a three-dimensional system. This behavior can be interpreted by a low dimensionality of the three-dimensional oxide-coated cluster assemblies because of a porous cluster stacking and imperfect or non-uniform oxide shell.

1 Introduction

Recently there has been growing interest in obtaining various nanostructured materials by using different preparation methods and understanding their novel physical properties, being significantly different from those for the corresponding bulk counterparts [1, 2]. These physical properties also depend on crystalline size, shape, and dispersion of nanoparticles. A cluster-assembling method [3, 4], in which nanometer-size-controlled clusters are directly deposited on a substrate, is a promising alternative to fabricate nano-scale-controlled materials. We have fabricated Ni [5], Cr [6], and Co [7 to 9] cluster assemblies by a plasma-gas-condensation (PGC) type cluster beam deposition technique [10] and studied their physical properties and cluster–cluster coalescence behavior. In order to stabilize the cluster surface and minimize cluster–cluster coalescence, we have prepared CoO-coated Co cluster-assembled material. For this core-shell-type material, spin-dependent tunnel-type conductivity between ferromagnetic Co cores and enhanced magnetoresistance in the Coulomb blockade regime are found [11]. The absolute value of magnetoresistance ratio increases sharply with decreasing temperature: from 3.5% at 25 K to 20.5% at 4.2 K.

In this paper, we concentrate our attention on exploring structural and electronic properties in the oxide-coated metal cluster assemblies, which were obtained by light oxidization of cluster surfaces. The oxide-coated metal-cluster-assembled films are random or disorder systems in which the scale of randomness can be changed by the original cluster size and the degree of surface oxidation. For such a disorder system, the low temperature behavior of the resistivity is influenced by weak localization (WL) [12] and/or electron–electron interactions (EEI) [13]. There are different temperature dependence at low

[*] Corresponding author: e-mail: pengdl@mse.nitech.ac.jp

© 2003 WILEY-VCH Verlag GmbH & Co. KGaA, Weinheim 0031-8965/03/19604-0450 $ 17.50+.50/0

temperatures for two- and three-dimensional systems. At $T = 0$ K, a two-dimensional system cannot be a conductor, being an insulator. The scaling theory [12] predicts that at very low temperatures the sheet conductance σ of a metallic film deviates from its classic residual value σ_0 as

$$\sigma = \sigma_0 - (Pe^2/\pi h) \log T \,, \qquad (1)$$

where P is a number of order unity. The EEI effect in a disorder potential also results in a similar logarithmic temperature dependence [13]. Consequently there is no difference between WL and EEI pictures for two-dimensional systems at very low temperature. In the present oxide-coated metal cluster-assembled films, we observed that with increasing the degree of oxidation, the temperature dependence of the resistivity changes from a weak localization type to a strong localization type, and finally to tunneling type. In particular, we observed that the resistivity has the $\ln T$ dependence at low temperatures although the oxide-coated metal-cluster-assembled films are clearly three-dimensional.

2 Experimental

The samples were prepared by the PGC-type cluster beam deposition apparatus, whose detail was described elsewhere [5, 7], which is mainly composed of three parts: a sputtering chamber, a cluster growth room and a deposition chamber. We introduced oxygen gas through a nozzle set near the skimmer into the deposition chamber to form metallic oxide layers covering the clusters before depositing on the substrate. This process ensures that all clusters are oxidized before the cluster assemblies are formed. For constant R_{Ar} or $R_{Ar} + R_{He}$ (R_{Ar}: Ar gas flow rate; R_{He}: He gas flow rate), the gas pressure in the deposition chamber can be adjusted by changing R_{O_2}. We can also control the cluster size by changing R_{Ar} and R_{He}. Cluster-assembled films with the different effective thickness t, as measured by a quartz thickness monitor, were formed at room temperature on glass substrates with two pre-coated Au electrodes. Using the conventional four-probe method, the electrical resistivity was measured at a constant current. Transmission electron microscopy (TEM) and scanning electron microscopy (SEM) was used to study the cluster size, cluster stack structure and cross-sectional morphology of the cluster-assembled films.

3 Results

3.1 Cluster size and cross-sectional morphology

The initial stage of the clusters deposited on microgrids were observed by a Hitachi HF-2000 TEM, operating at 200 kV. Figure 1 shows bright field TEM images in the initial stage of the Co, Cr, and Ti clusters assemblies with effective thickness $t \approx 2.5$ nm. We estimated the cluster size distributions from digitized images recorded by a slow scan CCD camera in the object area of 350×350 nm^2 using an image-analysis software (Image-Pro PLUS: Media Cybernetics). As shown in Fig. 1, the mean cluster diameters are $d = 13$, 8, and 12 nm for the Co, Cr, and Ti clusters assemblies, respectively. We also observed the morphology of the cluster-assembled film with a high resolution SEM (JEOL: JSM-6320F) operating at 3 kV. Figure 2 shows cross-sectional SEM images of the Co-cluster-assembled film with $d = 13$ nm. We observed a near-random stacking of the Co clusters while did not detect “fingerlike structure” obtained by two-dimensional simulation of a “sticky ball” deposition for a very low kinetic energy cluster deposition [14], and columnar structure (texture) which has been observed in the films deposited by conventional thermal evaporation and sputtering. Moreover, individual Co clusters are distinguishable. This suggests that the Co clusters in the assemblies maintain their original size at room temperature. In addition, the actual thickness estimated from the cross-sectional SEM image is about $t_a = 540$ nm, while the effective thickness estimated from the thickness monitor was $t_e = 140$ nm, i. e. t_a is about four times of t_e. This implies that the cluster-assembled films are very porous.

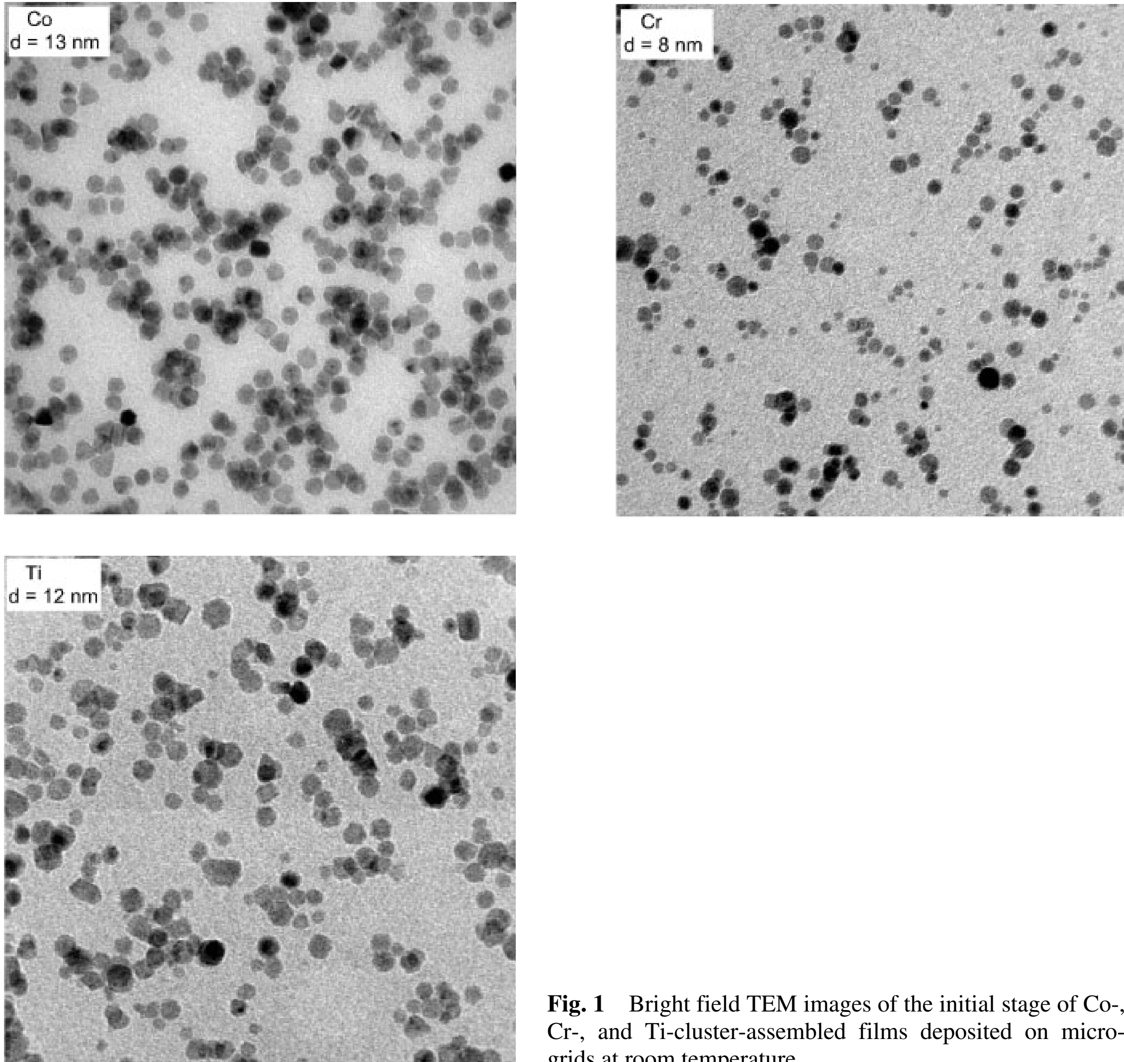

Fig. 1 Bright field TEM images of the initial stage of Co-, Cr-, and Ti-cluster-assembled films deposited on micro-grids at room temperature.

3.2 Temperature dependence of electrical resistivity

Figures 3a and 3b show the electrical resistivity, ρ, as a function of temperature, T, for the Co- and Cr-cluster-assembled films with $t_e = 100-200$ nm prepared at different R_{O_2}. As one can see from Fig. 3, with increasing R_{O_2}, there is the same tendency in the temperature dependence of ρ for both Co and Cr samples. For low R_{O_2}, the resistivity exhibits a minimum at temperature, T_{min}, which shifts to higher temperatures with increasing R_{O_2}. Above T_{min}, the samples show the metallic behavior as revealed by the linear T dependence of ρ. For high R_{O_2}, the resistivity minimum disappears and the temperature coefficient of resistivity is negative below room temperature. For higher R_{O_2}, such as $R_{O_2} = 0.35$ sccm for the Co cluster sample, we find a linear correlation between log σ and $1/T$, as well as the large magnetoresistance effect in the range of $T < 80$ K [11]. In this case, it has been confirmed that tunnel-type conduction appears. Moreover, it should be noted that the Cr cluster assemblies show the same temperature dependence of ρ for much lower R_{O_2} in comparison with the Co cluster assemblies. As we will show in the later, Ti cluster assemblies show the same behavior for the lowest R_{O_2}, while Cu samples show ordinary metal-

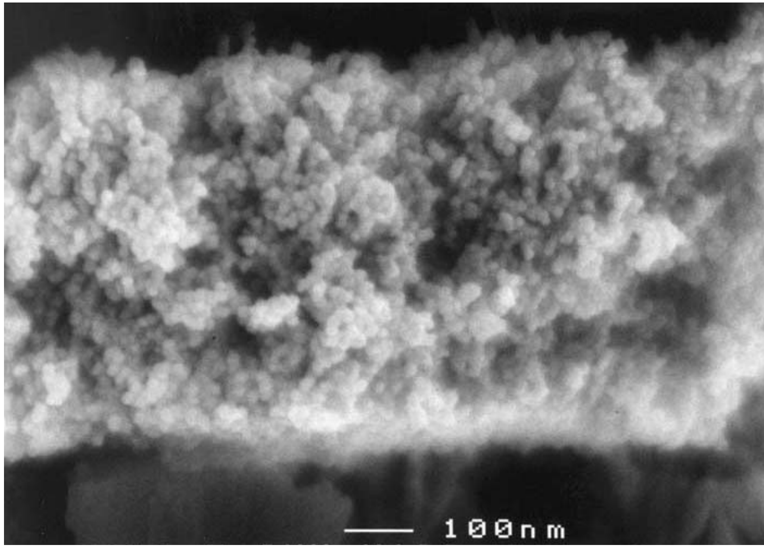

Fig. 2 Coss-sectional SEM image of the Co-cluster-assembled film with the mean cluster diameter, d = 13 nm. The effective thickness of the deposited film is t_e = 140 nm.

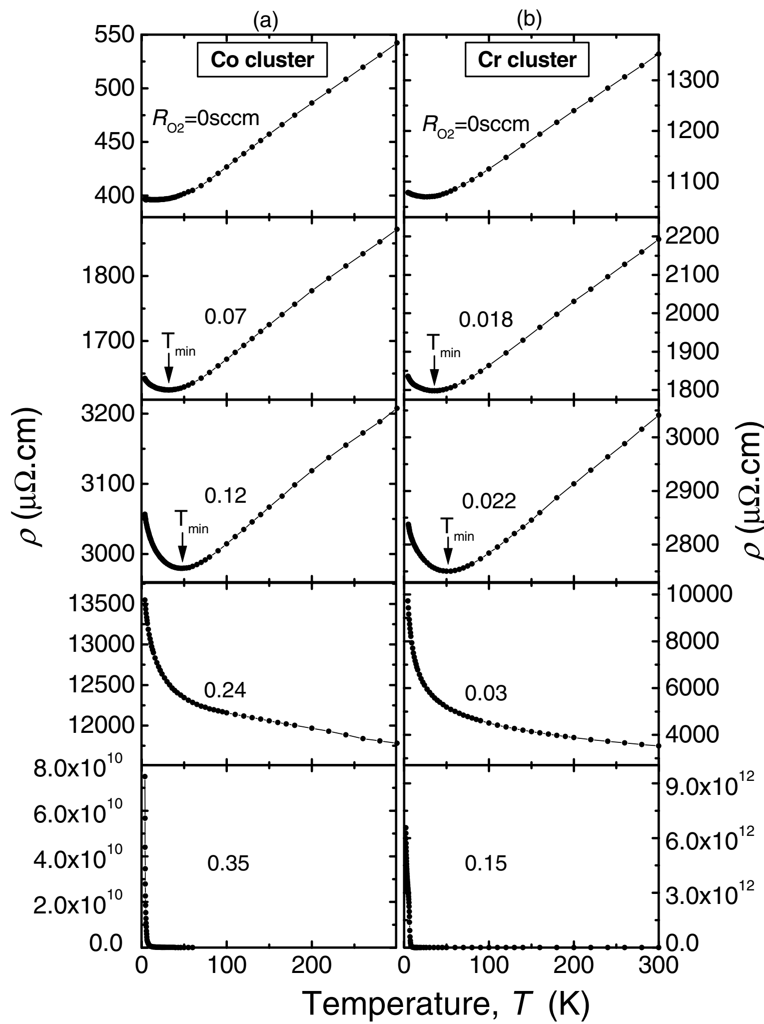

Fig. 3 Electrical resistivity, $\rho(T)$, as a function of temperature, T, for core-shell type Co- and Cr-cluster-assembled films prepared at different oxygen gas flow rate R_{O_2}.

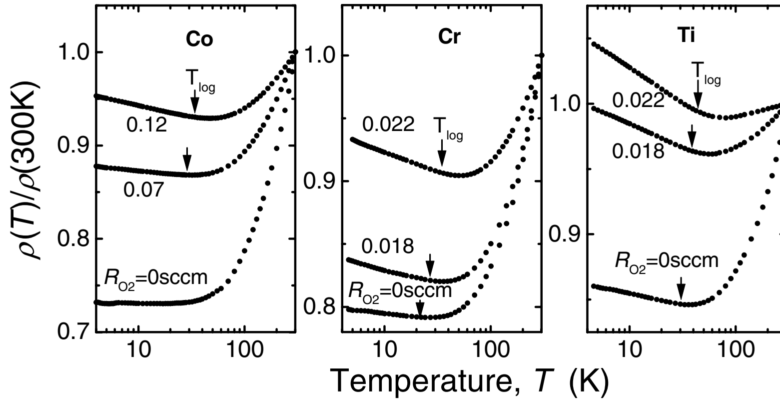

Fig. 4 Reduced resistivity, $\rho(T)/\rho(300\ \text{K})$, vs. log T for Co-, Cr-, and Ti-cluster-assembled films prepared at different oxygen gas flow rate R_{O_2}.

lic temperature dependence up to R_{O_2} = 1 sccm. These differences are attributable to the cohesive energy (ΔH) at room temperature for Co, Cr, and Ti oxides: $|\Delta H_{CoO}| < |\Delta H_{Cr_2O_3}| < |\Delta H_{TiO_2}|$ [15].

Figure 4 shows ρ normalized to the resistivity at T = 300 K as a function of the logarithm of T for the Co, Cr, and Ti cluster assemblies prepared at low different R_{O_2}. The overall resistivities exhibit ln T dependence below T_{log}. The value of ρ logarithmically increases with decreasing T and the increase rate of $\rho(T)$ becomes more pronounced with increasing R_{O_2}.

Figures 5 show the sheet resistance, R_{sheet}, vs log T for the Cr-cluster-assembled films with t = 30, 300, and 600 nm prepared at R_{O_2} = 0.022 sccm. As one can see here, the sheet resistance clearly reveals the characteristic low temperature dependence: R_{sheet} has a ln T behavior expected for a two-dimensional disorder system.

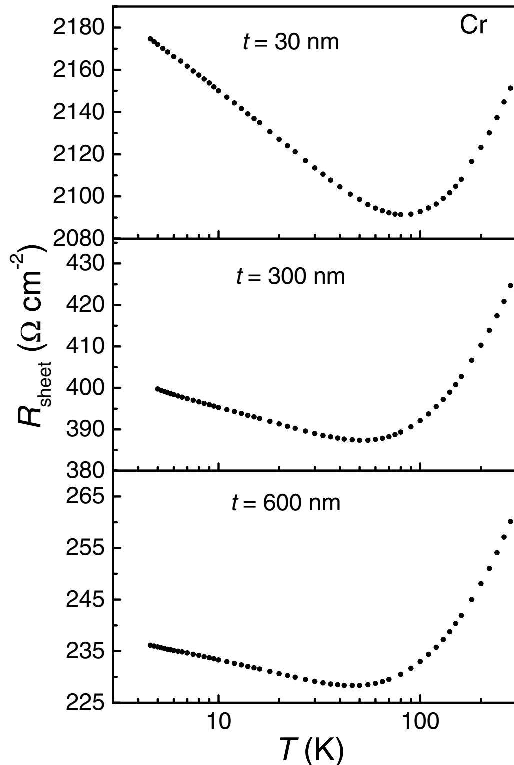

Fig. 5 Sheet resistance, R_{sheet}, vs log T for the Cr-cluster-assembled films with t = 30, 300, and 600 nm prepared at R_{O_2} = 0.022 sccm.

3.3 Magnetoresistance effect

Figure 6 shows the magnetic field (parallel to the film plane) dependence of the normalized magnetoresistance at 5 K for the Co-, Cr- and Ti-cluster-assembled films with t = 200 nm prepared at R_{O_2} = 0.12, 0.022 and 0.022 sccm, respectively. As shown here, the magnetoresistance exhibits positive contributions up to H = 50000 Oe for the Cr and Ti samples and up to 5000 Oe for the Co sample. It becomes negative for the Co sample when H > 5000 Oe. Tangent of the magnetoresistance is negative for the Cr sample H > 4000 Oe and does not become negative up to H = 50000 Oe for the Ti sample.

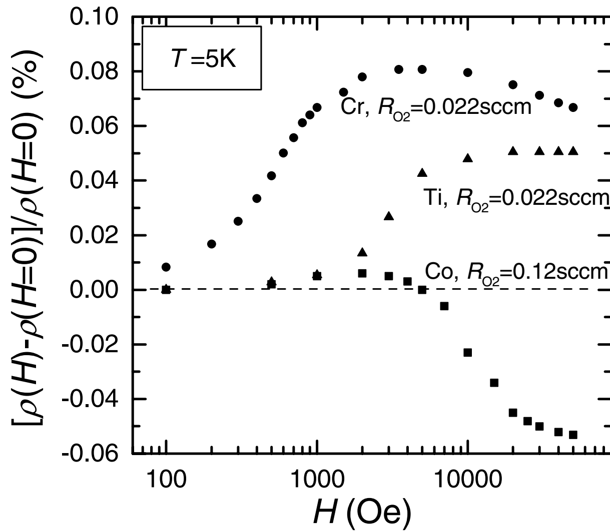

Fig. 6 Magnetic field dependence of the magnetoresistance ratio, $MR = (\rho_H - \rho_0)/\rho_0$, at 5 K for the oxide-coated Co-, Cr- and Ti-cluster-assembled films prepared at R_{O_2}= 0.12, 0.022 and 0.022 sccm, respectively.

4 Discussion

As described in Section 3.2, there is clear ln T dependence of the resistivity for Co, Cr and Ti cluster assemblies prepared under very low R_{O_2}. With regard to the logarithmic temperature dependence and a resistivity minimum, there have been many reports, such as Al/Ni [16], Mo/Ni [17] and Nb/Ni [18] multilayers, Co–Al–O [19], Pd–C [20] granular films, etc. The transport behavior observed for these systems is interpreted by a weak localization effect [16–20] and an electron–electron interaction [20]. The WL [12] and EEI [13] theories, however, predicted that ρ varies linearly with ln T for a two-dimensional disordered system. They are not applied for three-dimensional systems in which the sample thicknesses are more than one order of magnitude larger than the cluster size. As shown in Fig. 5, the ln T behavior is manifested for t_e = 30 nm and is depressed with increasing t_e though it is remarkably maintained up to t_e = 600 nm. According to our cross-sectional TEM observation of the cluster-assembled film (Fig. 2), the actual thickness t_a is about four times larger than the effective thickness t_e due to the particular porous structure of the cluster-assembled film. This means that the sheet resistance still exhibits the ln T behavior up to the actual thickness of about t_a = 2400 nm (t_e = 600 nm) which is more than two order of magnitude larger than the cluster size (d = 8 nm).

To judge the dimensionality, we need to estimate the following two characteristic lengths. One is the length L_ϕ over which the electrons can travel without losing their phase memories and is given by

$$L_\phi = (D\tau_\phi)^{1/2}\,, \tag{2}$$

where τ_ϕ is the phase relaxation time and D is the diffusion constant which is given by $D = \upsilon_F l_e/3$ with υ_F as Fermi velecity and l_e representing the electronic mean free path for elastic scattering. L_ϕ is a measure for the dimensionality of the WL effect because it arises from interference. The other is the thermal length L_T which is responsible for the Coulomb interaction effect and is given by

$$L_T = (Dh/k_B T)^{1/2}\,, \tag{3}$$

where h is the Plank constant. L_T is a measure for the dimensionality of the EEI effect. When film thickness $t < L_\phi$ and L_T, the sample is two-dimensional. Using Eq. (2) and (3), we estimate the dimensionality of our samples. For metal, $\upsilon_F \sim 10^6$ m s^{-1}, $l_e \sim 10^8$ m, and $D \sim 10^{-2}$ m s^{-1}, we typically calculate the characteristic lengths L_ϕ = 100 nm and L_T = 70 nm, respectively, for $\tau_\phi = 10^{-12}$ s [21] and at T = 10 K. The actual thickness of the sample (t_a = 2400 nm) is one order of magnitude larger than L_ϕ and L_T, implying

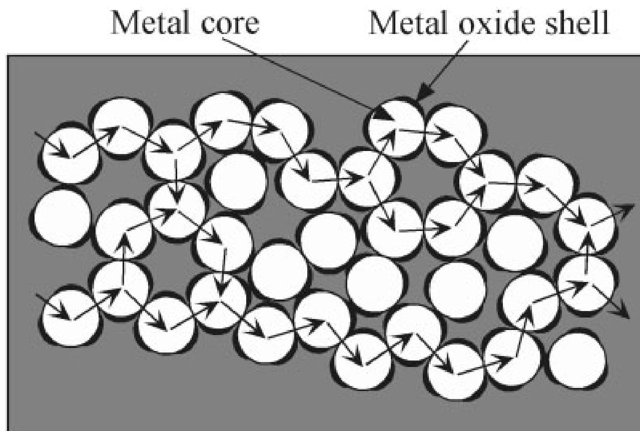

Fig. 7 A schematic structure model of the oxide-coated metal-cluster-assembled films prepared at very low R_{O_2} region.

that the sample should be three-dimensional. Indeed, the same logarithmic behavior was also observed for other systems, which are unquestionably three-dimensional [22–24]. As can see from Fig. 2, the films are very porous and individual clusters are distinguishable. This situation is schematically shown in Fig. 7, based upon the high resolution TEM observation: the Co clusters prepared at higher R_{O_2} were covered with thicker CoO shells composed of very small crystallites. In the case of the low R_{O_2}, the amount of the oxide formed should be very small and the oxide layers do not coat core clusters perfectly. In this case, adjacent clusters can form chains (network) with quasi-metallic contact (i.e., either with metallic "point" connections or with very thin insulating oxide barriers with negligible activation energy). The electrons travel only by the limited paths with the smallest resistance. It has been discussed that a three-dimensional cluster-assembled system has a fractal dimension at the percolation threshold [25]. In this context, the logarithmic temperature dependence of the resistivity at low temperatures can be ascribed to the WL and/or EEI effects in a false-low-dimensional system.

Looking at Figs. 3a and 3b, for the Co sample with R_{O_2} = 0.24 sccm and the Cr sample with R_{O_2} = 0.03 sccm, the temperature coefficient of resistivity becomes negative below room temperature and the resistivity minimum disappears. This suggests that the metallic or quasi-metallic conduction path of Co and Cr clusters is completely broken by the insulating oxide shells and then the electrical current flows by thermal hopping or tunneling. For clarifying this point, we have attempted the following plots for the temperature dependence of ρ: ln ρ versus T^{-1}, ln ρ versus $T^{-1/2}$, and ln ρ versus $T^{-1/4}$ which represent the semiconductor-type conductance in crystalline semiconductors, tunnel-type conductance in insulating granular [19, 26], and variable range hopping conductance in amorphous semiconductors [27], respectively. Figure 8 shows such plots for the oxide-coated Co- and Cr-cluster-assembled films. It indicates that the plot of ln ρ versus $T^{-1/4}$ for variable range hopping conductance in amorphous semiconductors is most appropriate.

The relation of ln ρ versus $T^{-1/4}$ was first derived by Mott by taking into account the conduction in amorphous semiconductors, in which the electron transport is dominated by the thermal hopping (i.e. phonon-assisted tunneling) between localized states which are randomly distributed with "traps"-potential fluctuation. The electron can jump from a localized state to a neighboring one, where their wave functions overlap each other. The difference in the eigen state energies is compensated by the absorption or emission of phonons. This mechanism is valid when the electron coherence length is longer than the localization length, namely for a strongly localized disorder system. This type of conduction is also very different from that in semiconductors in which the density of states at Fermi level is zero. In an Anderson-localization type insulators, however, the density of states at the Fermi level is finite. For the Co and Cr cluster assemblies prepared under low R_{O_2} (for Co: R_{O_2} = 0.24 sccm; for Cr: R_{O_2} = 0.03 sccm), thin oxide layers may be of highly disordered structure and have the localized states described by Mott's model, leading to the relation of ln ρ versus $T^{-1/4}$.

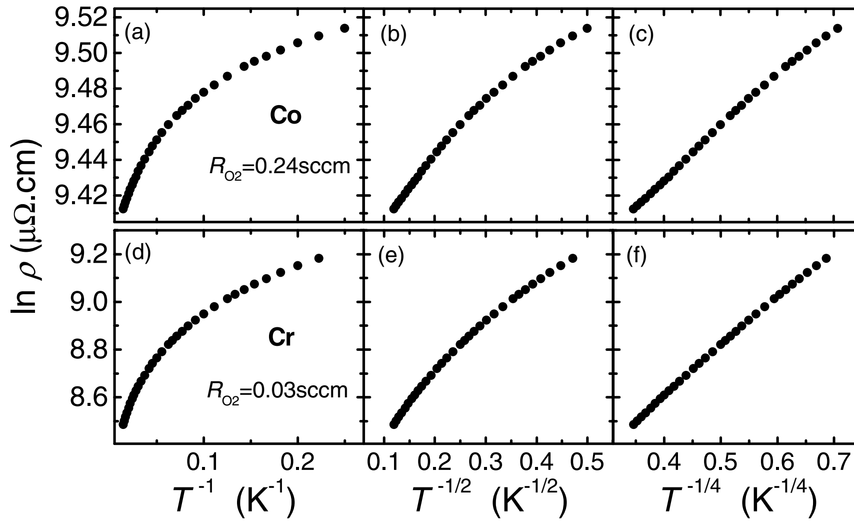

Fig. 8 Temperature dependence of electrical resistivity (ρ) for a Co-cluster-assembled film with R_{O_2} = 0.24 sccm and a Cr-cluster-assembled film with R_{O_2} = 0.03 sccm plotted by ln ρ versus T^{-1}, ln ρ versus $T^{-1/2}$, and ln ρ versus $T^{-1/4}$, respectively.

As R_{O_2} is further increased, the oxide layers become thicker and crystalline. Consequently, a tunnel-type temperature dependence of ln ρ versus T^{-1} was observed below $T = 80$ K for the CoO-coated mono-dispersed Co cluster assemblies with $R_{O_2} > 0.3$ sccm [11]. This differs from the well-known temperature dependence of log ρ vs. $1/T^{1/2}$ for disordered granular materials prepared by precipitation from supersaturated solid systems [26].

5 Conclusion

We have shown various conductivity behaviors in these oxide-caoted metal cluster-assembled films with changing the oxygen gas flow rate (R_{O_2}). In the case of the Co-, Cr-, and Ti-cluster-assembled films, there is the same tendency in the temperature dependence of ρ with increasing R_{O_2}. For low R_{O_2}, the resistivity exhibits a minimum at T_{min} and shows ln T dependence below T_{min} due to the WL and/or EEI effects of conduction electrons in disordered thin oxide shells covering metal cores. Above T_{min}, the samples show the metallic behavior as revealed by the linear temperature dependence of ρ. It is found that the ln T dependence still remains for the thick oxide-caoted metal cluster-assembled films (actual thickness t_a = 2400 nm) which is clearly a three-dimensional system. This behavior can be interpreted by the low dimensionality of the infinite cluster network in the three-dimensional cluster assemblies due to non-uniform oxide shell for the low R_{O_2} and the porous structure of the cluster assemblies. With further increasing R_{O_2}, the resistivity minimum disappears and the temperature coefficient of resistivity is negative below room temperature. The resistivity exhibits the temperature dependence of ln ρ versus $T^{-1/4}$, probably due to the presence of the strongly localized states in disordered thin oxide shells. For higher R_{O_2}, such as R_{O_2} = 0.35 sccm for the Co cluster, the tunnel-type conduction between the metal cluster cores is observed.

Acknowledgments This work has been supported by Core Research for Evolutional Science and Technology (CREST) of Japan Science and Technology Corporation (JST). One of the authors (D. L. Peng) appreciates the financial support from Japan Society for the Promotion of Science (JSPS).

References

[1] D. L. Leslie-Pelecky and R. D. Rieke, Chem. Mater. **8**, 1770 (1996).
[2] Nanomaterials: Synthesis, properties and Applications, edited by A. S. Edelstein and R. C. Cammarata (Institute of Physics, Bristol, 1996).
[3] P. Melinon, V. Paillard, V. Dupuis, A. Perez, P. Jensen, A. Hoareau, M. Broyer, J. L. Vaille, M. Pellarin, B. Baguenard, and J. Lerme, Int. J. Mod. Phys. B **9**, 339 (1995).
[4] A. Perez, P. Melinon, V. Dupuis, P. Jensen, B. Prevel, J. Tuaillon, L. Bardotti, C. Martet, M. Treilleux, M. Broyer, M. Pellarin, J. L. Vaille, B. Palpant, and J. Lerme, J. Phys. D: Appl. Phys. **30**, 709 (1997). [3]F. J. Darnell, J. Appl. Phys., 32, 186 S. (1961).
[5] T. Hihara and K. sumiyama, J. Appl. Phys. **84**, 5270 (1998).
[6] S. Yamamuro, K. Sumiyama, and K. Suzuki, J. Appl. Phys. **85**, 483 (1999).
[7] S. Yamamuro, K. Sumiyama, T. Hihara, and K. Suzuki, J. Phys.: Condens. Matter **11**, 3247 (1999).
[8] S. Yamamuro, K. Sumiyama, T. Kamiyama, and K. Suzuki, J. Appl. Phys. **86**, 5726 (1999);
[9] D. L. Peng, T. J. Konno, K. Wakoh, T. Hihara, and K. Sumiyama, Appl. Phys. Lett. **78**, 1535 (2001).
[10] H. Haberland, M. Karrais, M. Mall, and Y. Thurner, J. Vac. Sci. Technol. A **10**, 3266 (1992).
[11] D. L. Peng, K. Sumiyama, S. Yamamuro, T. Hihara, and T. J. Konno, Appl. Phys. Lett. **74**, 76 (1999).
[12] E. Abrahams, P. W. Anderson, D. C. Licciardello, and T. V. Ramakrishnan, Phys. Rev. Lett. **42**, 673 (1979).
[13] B. L. Alt'shuler, A. G. Aronov, and P. A. Lee, Phys. Rev. Lett. **44**, 1288 (1980).
[14] H. Haberland, M. Mall, M. Moseler, Y. Qiang, T. Reiners, and Y. Thurner, J. Vac. Sci. Technol. A **12**, 2925 (1994).
[15] Physical Chemistry of Metals, edited by L. S. Darken and R. W. Gurry (McGraw Hill, New York, 1953).
[16] H. Sato, I. Sakamoto, and C. Fierz, J. Phys.: Condens. Matter **3**, 9067 (1991).
[17] C. Uher, R. Clarke, G. Zheng, and I. K. Schuller, Phys. Rev. B **30**, 453 (1984).
[18] M. T. Perez and J. L. Vicent, Phys. Rev. B **38**, 9503 (1988).
[19] H. Fujimori, S. Mitani, S. Ohnuma, T. Ikeda, T. Shima, and T. Masumoto, Mater. Sci. Eng. **A181/A182**, 897 (1994).
[20] A. Carl, G. Dumpich, and D. Hallfarth, Phys. Rev. B **39**, 915 (1989);
Phys. Rev. B **39**, 3015 (1989); Thin Solid Films **193/194**, 1065 (1990).
[21] I. L. Aleiner, B. L. Altshuler, and M. E. Gershenson, Waves Random Media, **9**, 201 (1999).
[22] C. C. Tsuei, Solid State Commun. **27**, 691 (1978).
[23] G. Deutscher, B. Bandyopadhyay, T. Chui, P. Lindenfeld, W. L. McLean, and T. Worthington, Phys. Rev. Lett. **44**, 1150 (1980).
[24] S. L. Weng et al., Phys. Rev. Lett. **50**, 1795 (1983).
[25] D. Stauffer, Phys. Rep. **54**, 1 (1979)
[26] P. Sheng, B. Abeles, and Y. Arie, Phys. Rev. Lett. **31**, 44 (1973).
[27] N. F. Mott, J. Non-Cryst. Solids **1**, 1 (1969);
Conduction in Non-crystalline Materials (Clarendon, Oxford, 1987) p. 27.